Journal of Statistical Physics, Vol. 56, Nos. 1/2, 1989

Computer Simulation of Some Dynamical Properties of the Lorentz Gas

C. G. Joslin[1] **and P. A. Egelstaff**[1]

Received February 4, 1988; final December 12, 1988

We carried out molecular dynamics simulations of a Lorentz gas, consisting of a lone hydrogen molecule moving in a sea of stationary argon atoms. A Lennard-Jones form was assumed for the H_2–Ar potential. The calculations were performed at a reduced temperature $T^* = kT/\varepsilon_{H_2\text{-Ar}} = 4.64$ and at reduced densities $\rho^* = \rho_{Ar}\sigma_{Ar}^3$ in the range 0.074–0.414. The placement of Ar atoms was assumed to be random rather than dictated by equilibrium considerations. We followed the trajectories of many H_2 molecules, each of which is assigned in turn a velocity given by the Maxwell–Boltzmann distribution at the temperature of the simulation. Solving the equations of motion classically, we obtained the translational part of the incoherent dynamic structure factor for the H_2 molecule, $S_{tr}(q, \omega)$. This was convoluted with the rotational structure factor $S_{rot}(q, \omega)$ calculated assuming unhindered rotation to obtain the total structure factor $S(q, \omega)$. Our results agree well with experimental data on this function obtained by Egelstaff *et al.* At the highest density ($\rho^* = 0.414$) we studied the dependence of $S(q, \omega)$ on system size (number of Ar atoms), number of H_2 molecules for which trajectories are generated, and the length of time over which these trajectories are followed.

KEY WORDS: Lorentz gas; molecular dynamics; simulation; neutron scattering; dynamic structure factor; intermediate structure function.

1. INTRODUCTION AND THEORY

In this paper we report molecular dynamics (MD) simulations of a hydrogen–argon mixture. The Ar atom mass is so much greater than that of the H_2 molecule (by a factor of 20) that to a first approximation it is valid to regard the Ar atoms as fixed. At low densities of H_2, the H_2–H_2 interaction can be neglected, so that the H_2 molecule motion is that of a

---

[1] Department of Physics, University of Guelph, Guelph, Ontario N1G 2W1, Canada.

single particle scattering from an array of fixed centers of force. This is an example of a "Lorentz gas."(1) We assume the intermolecular (H_2–Ar) potential is of the Lennard-Jones (LJ) form

$$u_{\mathrm{H_2\text{-}Ar}}(r) = 4\varepsilon_{\mathrm{H_2\text{-}Ar}}[(\sigma_{\mathrm{H_2\text{-}Ar}}/r)^{12} - (\sigma_{\mathrm{H_2\text{-}Ar}}/r)^6] \tag{1}$$

where $\varepsilon_{\mathrm{H_2\text{-}Ar}} = 64$ K and $\sigma_{\mathrm{H_2\text{-}Ar}} = 3.168$ Å.(2) Most of our simulations are performed at a temperature of 297 K and a density (ρ_{Ar}) of $10.5 \times 10^{27}\ \mathrm{m}^{-3}$, corresponding to a reduced temperature $T^* = kT/\varepsilon_{\mathrm{H_2\text{-}Ar}} = 4.64$ and a reduced density $\rho^* = \rho_{\mathrm{Ar}}\sigma_{\mathrm{Ar}}^3 = 0.414$ ($\sigma_{\mathrm{Ar}} = 3.405$ Å). These correspond to a state for which experimental data are available. Some calculations were also performed at lower densities, $\rho^* = 0.074$, 0.154, and 0.282.

Rather than using a many-body MD program to generate equilibrium configurations of Ar atoms, we have assumed that these are randomly placed (we do not expect this to alter significantly any of the main results or conclusions of this paper, and in fact a comparison of our results with earlier work employing equilibrium configurations(2) shows close agreement; see Fig. 8). We then study successively the motion of many (up to 1000) H_2 molecules in this fixed bath of scatterers, by solving classically the translational equations of motion [with the intermolecular potential of Eq. (1), the H_2 rotational motion is unhindered]. A Verlet algorithm was used.(3) The initial velocities of the H_2 molecules were assigned randomly, but in accord with Maxwell–Boltzmann statistics at the temperature of the computer experiment. The subsequent motion of these molecules was followed over up to 20,000 time steps [$\Delta t = 0.02\,\tau$, where $\tau = (M_{\mathrm{H_2}}\sigma_{\mathrm{H_2\text{-}Ar}}^2/48\varepsilon_{\mathrm{H_2\text{-}Ar}})^{1/2} = 8.90 \times 10^{-14}$ sec is the relaxation period of the motion]. Minimum-image periodic boundary conditions were employed.(4) The size of the central simulation cell was adjusted in order to vary the number of Ar atoms in the range $N_{\mathrm{Ar}} = 400$–2500.

The simulations yield the value of the intermediate structure function $F_{\mathrm{tr}}(q, t)$ and its Fourier transform $S_{\mathrm{tr}}(q, \omega)$, the (translational) incoherent dynamic structure factor:

$$\begin{aligned} F_{\mathrm{tr}}(q, t) &= \langle \exp[-i\mathbf{q}\cdot\mathbf{r}(0)]\exp[i\mathbf{q}\cdot\mathbf{r}(t)]\rangle \\ &= \langle j_0(qR(t))\rangle \end{aligned} \tag{2}$$

$$S_{\mathrm{tr}}(q, \omega) = \frac{1}{2\pi}\int_{-\infty}^{+\infty} F_{\mathrm{tr}}(q, t)e^{-i\omega t}\,dt \tag{3}$$

In Eq. (2), $R(t) = |\mathbf{r}(t) - \mathbf{r}(0)|$ is the displacement of the hydrogen molecule in time t, and $j_0(x) = (\sin x)/x$ is the zeroth-order spherical Bessel function.

In (2) and (3), $\hbar\mathbf{q}$ and $\hbar\omega$ (where $\hbar = h/2\pi$ is Planck's constant) may be interpreted respectively as the momentum and energy transfer to an H_2 molecule in neutron scattering.(2) Experimental data on the dynamic structure factor for the incoherent scattering of neutrons are available for H_2–Ar mixtures at the densities and temperature of the simulations,(5) and our results may be compared to this. We assume that molecular rotational and translational motion is uncoupled at our densities, so it is necessary to convolute the translational function $S_{\rm tr}(q, \omega)$ with the corresponding rotational function $S_{\rm rot}(q, \omega)$ calculated for the free molecule. This calculation is described by Young and Koppel(6) and we use their expression for $S_{\rm rot}(q, \omega)$. We have

$$S(q, \omega) = \int_{-\infty}^{+\infty} S_{\rm tr}(\omega')\, S_{\rm rot}(\omega - \omega')\, d\omega' \tag{4}$$

$S(q, \omega)$ is normalized so that

$$\int_{-\infty}^{+\infty} S(q, \omega)\, d\omega = 1 \tag{5}$$

A major aim of this work is to investigate in some detail the dependence of $S(q, \omega)$ (and by implication that of other functions containing dynamical information) on various parameters of the simulation. These include the system size $N_{\rm Ar}$, the duration of the simulation, and the number of H_2 molecules whose motion is studied. A number of conclusions on the importance of these parameters will be drawn from the results.

2. CALCULATIONS AND RESULTS

The simulations were performed on the Ontario Universities Cray X-MP/22 supercomputer, and required, in total, approximately 25 h of CPU time. For the highest density, $\rho^* = 0.414$, three system sizes, $N_{\rm Ar} = 400$, 1000, and 2500 particles, were studied, and for each the simulation was run for both 5000 and 20,000 time steps (i.e., for about 10 and 40 psec, respectively). In each of these cases the trajectories of either 100 or 1000 H_2 molecules were generated and followed. By observing the displacement $R(t)$ as a function of time, $S(q, \omega)$ was computed as described in Section 1 for five different values of $q = 0.5$, 0.7, 1, 1.5, and 2 Å^{-1}, and over the whole range of frequencies ω for which it is appreciable (about 5 meV at 0.5 Å^{-1}, and 30 meV at 2 Å^{-1}).

Our results for $N_{\rm Ar} = 2500$, 20,000 time steps and 1000 H_2 trajectories are displayed in Figs. 1–5, where they are compared with neutron

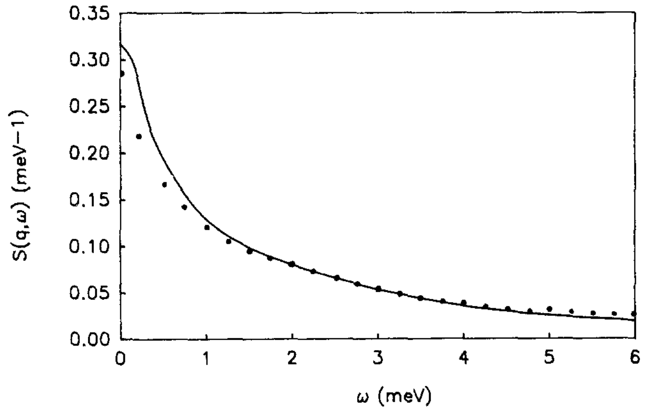

Fig. 1. The incoherent dynamic structure factor $S(q, \omega)$ as a function of frequency for $q = 0.5$ Å^{-1}. The simulation is shown by the line and the experimental data by solid circles ($\rho^* = 0.414$).

scattering data obtained by Egelstaff *et al.*(5) (we have deconvoluted the experimental resolution function(2) from these data). Agreement is on the whole very good. However, the simulation $S(q, \omega)$ decays rather too rapidly with ω. This is presumably because the Ar atom mass, although large compared to the H_2 mass, is not infinite, so that some degree of Ar atom motion occurs on the time scale of H_2 molecular motion. This effect is discussed in more detail in ref. 2. Also, the simulation curves show "peaking" at low frequencies. This effect reflects the oscillatory motion of an H_2 molecule which is nearly trapped in a rigid cage of Ar atoms.(7) The experimental curves show a much smaller effect, presumably because Ar

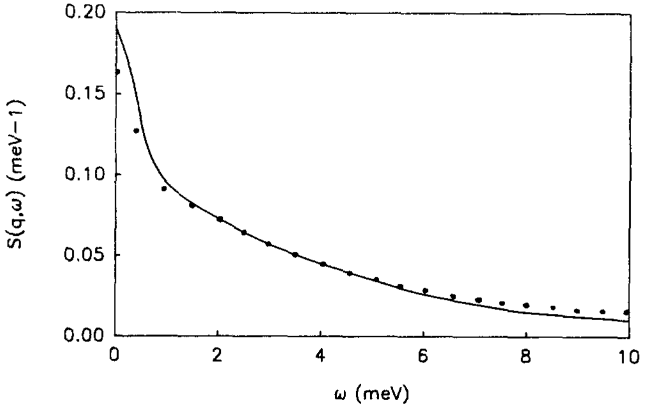

Fig. 2. The dynamic structure factor $S(q, \omega)$ for $q = 0.7$ Å^{-1} ($\rho^* = 0.414$).

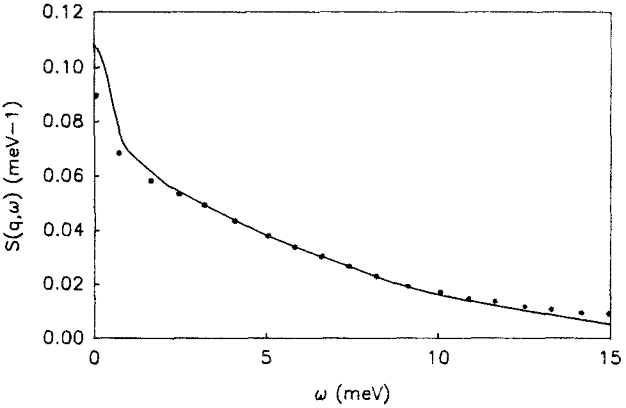

Fig. 3. The dynamic structure factor $S(q, \omega)$ for $q = 1\ \text{Å}^{-1}$ ($\rho^* = 0.414$).

atom motion eventually breaks up the cage, allowing the H_2 molecule to escape.

Figure 6 shows a plot of $qS_{\text{tr}}(q, \omega)$ vs. ω/q for various values of q. This graph clearly demonstrates departures from ideality, since for an ideal gas

$$qS_{\text{tr}}(q, \omega) = (M_{H_2}/2\pi kT)^{1/2} \exp[-(M_{H_2}/2kT)(\omega/q)^2] \tag{6}$$

is a universal function of ω/q, i.e., is independent of q. The behavior actually observed is that the zero-frequency amplitude $qS_{\text{tr}}(q, 0)$ increases with decreasing q, reflecting the diffusive character of H_2 molecule motion

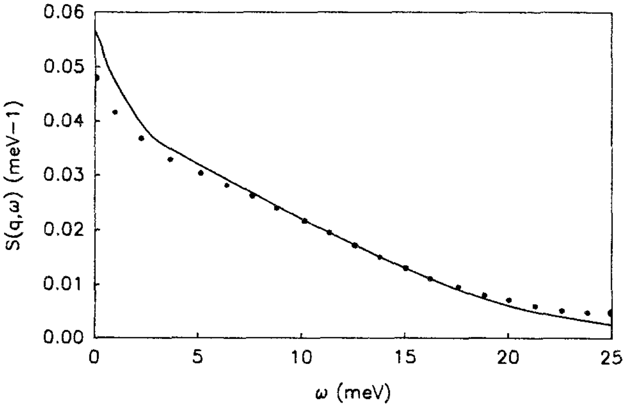

Fig. 4. The dynamic structure factor $S(q, \omega)$ for $q = 1.5\ \text{Å}^{-1}$ ($\rho^* = 0.414$).

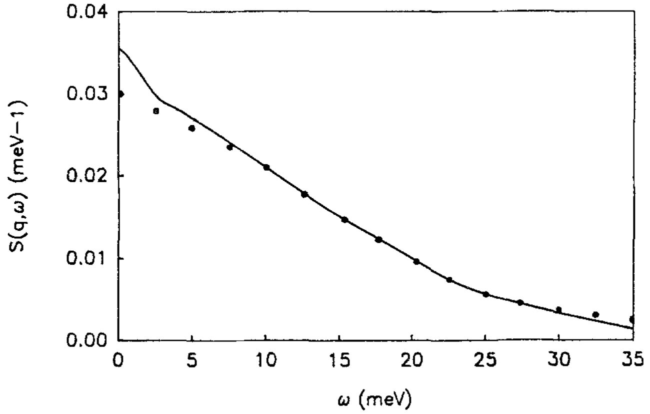

Fig. 5. The dynamic structure factor $S(q, \omega)$ for $q=2\,\text{Å}^{-1}$ ($\rho^*=0.414$).

at long times.[2] Figure 7 shows a plot of $F_{\text{tr}}(q, t)$ vs. qt for different q; the ideal gas result, which is

$$F_{\text{tr}}(q, t)=\exp\left(-\frac{1}{2}\frac{kT}{M_{H_2}}q^2t^2\right) \tag{7}$$

is also shown. For large t, $F_{\text{tr}}(q, t)$ lies significantly above this value, especially for small q, displaying a more exponential-like decay.[2]

Tables I and II show a comparison of the values of $F_{\text{tr}}(q, t)$ obtained

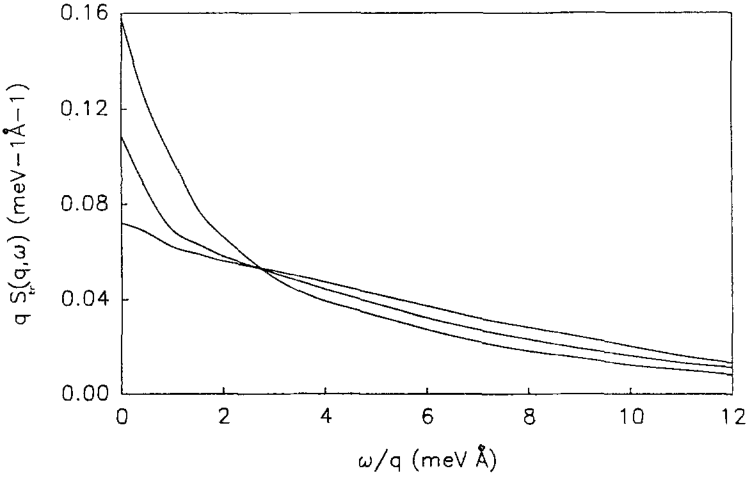

Fig. 6. Plot of $qS_{\text{tr}}(q, \omega)$ vs. ω/q for $q=0.5$, 1, 2 Å^{-1}. Amplitude at zero frequency increases as q decreases ($\rho^*=0.414$).

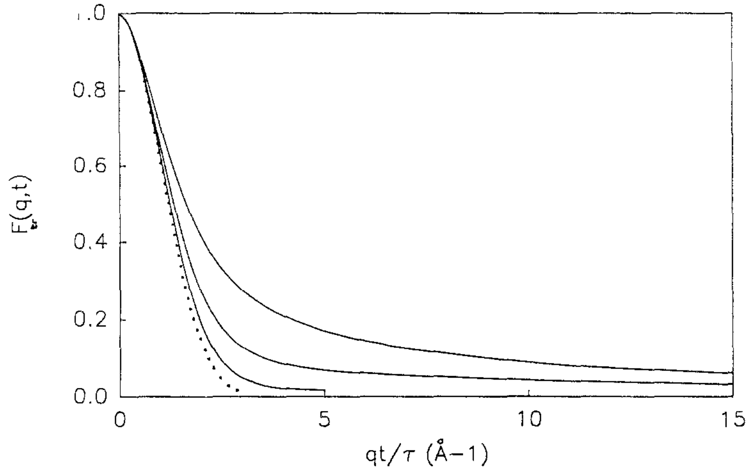

Fig. 7. Plot of $F_{tr}(q, t)$ vs. qt/τ for $q = 0.5$, 1, 2 Å^{-1}. Ideal gas result (dotted line) is also shown. Deviations from ideality increase as q decreases ($\rho^* = 0.414$).

Table I. The Intermediate Structure Function $F_{tr}(q, t)$ Computed from the Different Simulations, for Various Values of q[a]

	$F_{tr}(q, t)$		
N_{Ar}	$q = 0.5$ Å^{-1}	$q = 1$ Å^{-1}	$q = 2$ Å^{-1}
20,000 time steps, 1000 H_2 trajectories			
400	0.5013	0.5026	0.5035
1000	0.5065	0.5082	0.5097
2500	0.4947	0.4956	0.4967
5000 time steps, 1000 H_2 trajectories			
400	0.5013	0.5034	0.5047
1000	0.5025	0.5089	0.5113
2500	0.4920	0.4961	0.4973
20,000 time steps, 100 H_2 trajectories			
400	0.5218	0.5226	0.5229
1000	0.5432	0.5466	0.5492
2500	0.4516	0.4491	0.4483
5000 time steps, 100 H_2 trajectories			
400	0.5273	0.5271	0.5274
1000	0.5439	0.5512	0.5516
2500	0.4551	0.4538	0.4517

[a] For each case (for a particular value of q) t is the same. The values used are $t/\tau = 3.30$, 1.34, and 0.62 for $q = 0.5$, 1, and 2 Å^{-1}, respectively. At these times $F_{tr}(q, t)$ is approximately 1/2.

Table II. The Intermediate Structure Function $F_{tr}(q, t)$ Computed from the Different Simulations, for Various Values of q[a]

	$F_{tr}(q, t)$		
N_{Ar}	$q = 0.5$ Å^{-1}	$q = 1$ Å^{-1}	$q = 2$ Å^{-1}
20,000 time steps, 1000 H_2 trajectories			
400	0.05792	0.02465	0.008713
1000	0.05944	0.02505	0.009375
2500	0.06098	0.02677	0.009918
5000 time steps, 1000 H_2 trajectories			
400	0.06481	0.02667	0.009584
1000	0.06271	0.02445	0.008973
2500	0.06361	0.02545	0.007953
20,000 time steps, 100 H_2 trajectories			
400	0.07046	0.03454	0.01256
1000	0.07417	0.02918	0.00953
2500	0.04317	0.01589	0.00635
5000 time steps, 100 H_2 trajectories			
400	0.1042	0.04219	0.01302
1000	0.0798	0.02658	0.01029
2500	0.0500	0.02073	0.00553

[a] In each case (for a particular values of q) t is the same. The values used are $t/\tau = 30$, 20, and 10 for $q = 0.5$, 1, and 2 Å^{-1}, respectively. These times are well into the tail of $F_{tr}(q, t)$.

from the different simulations. Comparisons are given both for times at which this function has decayed to approximately one-half of its original value (of 1), and for much longer times in the "tail" of $F_{tr}(q, t)$.

3. DISCUSSION

The biggest variation in $F_{tr}(q, t)$ is seen on changing the number of H_2 trajectories. From Tables I and II we see this can be as much as 10% at the half-life, and 50% or more in the tail. (On the other hand, increasing the number of trajectories still further, to 5000, produces much smaller changes, on the order of 1%.) Clearly, to generate the proper Maxwell–Boltzmann statistics for the H_2 molecule's motion, it is necessary to follow about 1000 different randomly-generated trajectories; smaller numbers are inadequate. To quantify our understanding of this effect, we have measured the *effective* temperature T_{eff} for each simulation. This is defined by $\frac{3}{2}kT_{\text{eff}}=\frac{1}{2}M_{\text{H}_2}\langle v^2\rangle$, where $\langle v^2\rangle$ is the mean square velocity of the H_2 molecule averaged over all H_2 trajectories generated. Because the number of trajectories is finite, T_{eff} differs from the desired or "set" temperature $T=297$ K. For a system of 2500 Ar atoms followed over 20,000 time steps, we find $\delta T/T=(T_{\text{eff}}-T)/T=0.16$ and 0.03 for 100 and 1000 trajectories, respectively. Consider now how this error in temperature affects $F_{\text{tr}}(q, t)$. At short times, F_{tr} is approximately given by the ideal gas result, Eq. (7) (cf. Fig. 7). Thus, $F_{\text{tr}}=\exp(-\alpha T_{\text{eff}})$, where α is a constant (a function of q and t). At longer times, the H_2 molecular motion becomes diffusive, and $F_{\text{tr}}\approx\exp(-Dq^2t)$, where D is the diffusion constant.[2] For the state conditions studied D is roughly given by kinetic theory, i.e., $D\propto\sqrt{T_{\text{eff}}}$ approximately, so that here $F_{\text{tr}}=\exp(-\alpha'\sqrt{T_{\text{eff}}})$, where α' is another constant. In either case, an error δT in T leads to an error δF_{tr} in F_{tr} given by $\delta F_{\text{tr}}/F_{\text{tr}}\approx\delta T/T\ln F_{\text{tr}}$, to within a factor of 2. From Tables I and II this implies $\delta F_{\text{tr}}/F_{\text{tr}}\approx 0.11$ and 0.02 for 100 and 1000 trajectories, respectively, at the half-life of F_{tr}, and $\delta F_{\text{tr}}/F_{\text{tr}}\approx 0.6$ and 0.1 in the tail. These numbers agree very closely with the observed differences in F_{tr} from the 100- and 1000-trajectory simulations (see above, and also Tables I and II). We deem the errors at the 1000-trajectory level, $\approx 2\%$ at the half-life and $\approx 10\%$ in the tail, to be acceptable.

The next largest effect comes from changing the size of the system. With 1000 trajectories, there is about a 2% difference at the half-life in going from 1000 to 2500 Ar atoms. (For fewer trajectories, the effect is much more pronounced—about 20% for 100 trajectories.) In the tail, variations of about 10% are recorded as N_{Ar} varies. Note that these changes are *not* monotonic functions of N_{Ar}, nor is there any definite evidence of convergence at 2500 atoms.

The dependence of $F_{\text{tr}}(q, t)$ on N_{Ar} appears to be essentially independent of q (cf. Tables I and II). One expects some q dependence, but only at substantially smaller values of q. To see this, consider the following argument. Assuming diffusive behavior, $F_{\text{tr}}\approx\exp(-Dq^2t)$. Suppose we wish to observe the decay of F_{tr} to 2% of its initial value (unity). Then we must follow the motion of an H_2 molecule for a time of approximately $t=4/Dq^2$. In this time the molecule will diffuse, on average, a distance $\langle r^2\rangle^{1/2}=(6Dt)^{1/2}=(24)^{1/2}/q$. If $\langle r^2\rangle^{1/2}>\frac{1}{2}L$, where $L=(N_{\text{Ar}}/\rho_{\text{Ar}})^{1/3}$ is the size of the central MD simulation cell, a molecule which starts at the center of this cell will have moved into an image cell. Because of the periodic boundary conditions, its surroundings, and therefore its subsequent motion, will differ somewhat from those of a real (nonperiodic) system. This will introduce an error in the observed $F_{\text{tr}}(q, t)$ for $(24)^{1/2}/q>\frac{1}{2}L$ or $q\gtrsim 10/L$. For $N_{\text{Ar}}=400$, 1000, 2500 we have $L=34$, 46, 62 Å^{-1}, meaning that F_{tr} is in error for $q \lesssim 0.3$, 0.2, 0.15 Å^{-1}, respectively. In these simulations, however, $q \geqslant 0.5$ Å^{-1}, and this source of error will not be manifest, even for the smallest system studied.

The least important effect comes from changing the length of the simulation. Increasing the number of time steps from 5000 to 20,000 produces changes of less than 1% at the half-life and up to 20% in the tail of $F_{tr}(q, t)$. The corresponding change in the peak of $S(q, \omega)$ is approximately 1%. These findings are significant inasmuch as previous MD simulations of $F(q, t)$ and $S(q, \omega)$ have employed much longer runs. For example, both Schoen *et al.*(8) and Levesque *et al.*(9) simulated LJ liquid argon for 100,000 or more time steps (their Δt's are comparable to ours after scaling). Our results suggest that, in the case of a Lorentz gas, much shorter runs will suffice.

Figure 8 shows a comparison of our computed $F_{tr}(q, t)$ for $q = 1$ Å^{-1} with calculations by Sharma *et al.*(2) These authors simulated a Lorentz gas model of H_2–Ar assuming an equilibrium, rather than a random, placement of Ar atoms; however, rather few (~50) H_2 trajectories were followed. Agreement is very good and probably within the statistical uncertainty of the results in ref. 2. This indicates that the placement of the atoms of the host medium (Ar atoms) has a small effect on the dynamical behavior of the H_2 molecule, at fixed density.

Figure 9 shows the effect on $S_{tr}(q, \omega)$, for $q = 0.5$ Å^{-1}, of changing the Ar atom density. Simulations were performed at reduced densities

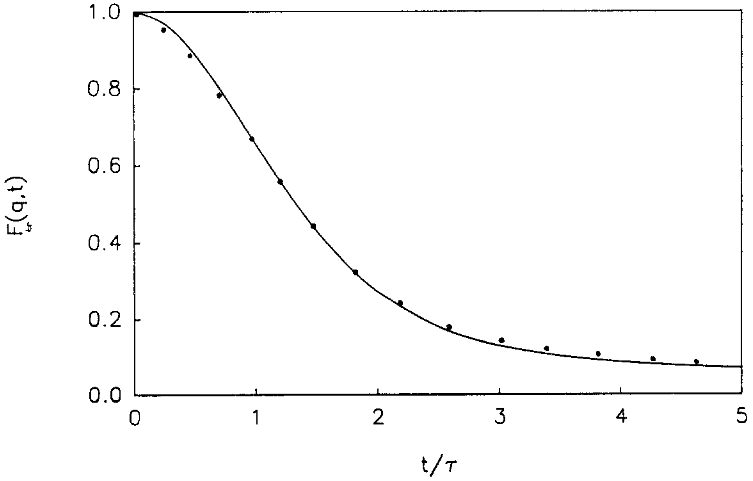

Fig. 8. Comparison of $F_{tr}(q, t)$ from this simulation (solid line) with earlier calculations by Sharma *et al.*(2) (dotted line), which assume an equilibrium, not a random, placement of Ar atoms. $q = 1$ Å^{-1} (data from ref. 2 were interpolated). ($\rho^* = 0.414$.)

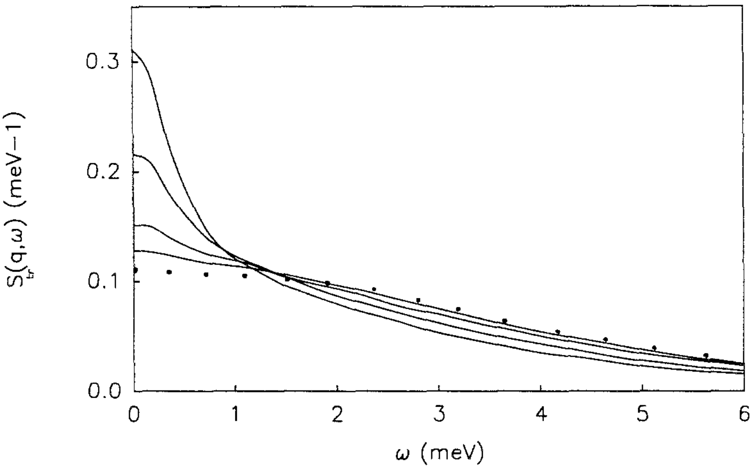

Fig. 9. Plot of $qS_{tr}(q, \omega)$ vs. ω/q for different densities ($\rho^* = 0.414$, 0.282, 0.154, 0.074); $q = 0.5$ Å^{-1}. Also shown is the ideal-gas result (dotted line). Deviations from ideality increase as ρ^* increases.

$\rho^* = 0.074$, 0.154, and 0.282 as well as $\rho^* = 0.414$. (T^* was kept constant at 4.64.) For these runs we took $N_{Ar} = 1000$, and followed 1000 H_2 trajectories for 5000 time steps. The data are strongly peaked at low frequencies, as a result of the long-time behavior of $F_{tr}(q, t)$. As the density is lowered, deviations from ideality (ideal gas result shown as dotted line) become less pronounced. For higher values of q, $S_{tr}(q, \omega)$ lies much closer to the ideal gas result, as expected.

4. SUMMARY

Molecular dynamics simulations of a Lorentz gas (H_2–Ar mixture with Lennard-Jones interaction) yield results for the dynamic structure factor $S(q, \omega)$ in good agreement with experiment for $q \geqslant 0.5$ Å^{-1}.

We have studied the dependence of simulated quantities on various parameters of the system, such as its size, the number of H_2 trajectories generated, and their duration. These studies show that while it is necessary to follow a fairly large number (about 1000) of trajectories, these can be of quite short duration (5000 time steps). Furthermore, reasonably small systems will suffice. For the current experimentally-accessible range of $q \geqslant 0.5$ Å^{-1}, 400 Ar atoms is large enough; should data become available at lower q, however, we anticipate that somewhat larger systems will be needed, requiring proportionately longer amounts of computer time. Interesting long-time dynamics may become apparent for these smaller values of q.

ACKNOWLEDGMENTS

We gratefully acknowledge the financial support of NSERC Canada, and the collaboration of the Ontario Centre for Large Scale Computation.

REFERENCES

1. S. Chapman and T. G. Cowling, *The Mathematical Theory of Non-Uniform Gases*, 3rd ed. (Cambridge University Press, 1970).
2. K. C. Sharma, S. Ranganathan, P. A. Egelstaff, and A. K. Soper, *Phys. Rev. A* **36**:809 (1987).
3. J. Kushick and B. J. Berne, in *Statistical Mechanics*, Vol. B, B. J. Berne, ed. (Plenum Press, New York, 1977), p. 41.
4. J. P. Valleau and S. G. Whittington, in *Statistical Mechanics*, Vol. A, B. J. Berne, ed. (Plenum Press, New York, 1977), p. 137.
5. P. A. Egelstaff, O. J. Eder, W. Glaser, J. Polo, B. Renker, and A. K. Soper, unpublished.
6. J. A. Young and J. U. Koppel, *Phys. Rev. A* **135**:603 (1964); V. Sears, *Proc. Phys. Soc.* **86**:953, 965 (1965).
7. W. Götze, E. Leutheusser, and S. Yip, *Phys. Rev. A* **25**:533 (1982).
8. M. Schoen, R. Vogelsang, and C. Hoheisel, *Mol. Phys.* **57**:445 (1986).
9. D. Levesque, L. Verlet, and J. Kürkijarvi, *Phys. Rev. A* **7**:1690 (1973).